Published in final edited form as:
Arthritis Rheum. 2013 December ; 65(12): 3176–3185. doi:10.1002/art.38174.

$P2X_7$ Blockade Attenuates Murine Lupus Nephritis by Inhibiting Activation of the NLRP3/ASC/Caspase 1 Pathway

Jijun Zhao, MD[1], **Hongyue Wang, MD**[1], **Chao Dai, PhD**[2], **Hongyang Wang, DDS, PhD**[2], **Hui Zhang, MD**[1], **Yuefang Huang, MD, PhD**[1], **Shuang Wang, MD, PhD**[1], **Felicia Gaskin, PhD**[2], **Niansheng Yang, MD, PhD**[1], and **Shu Man Fu, MD, PhD**[2]

[1]First Affiliated Hospital, Sun Yat-sen University, Guangzhou, China

[2]University of Virginia, Charlottesville

Abstract

Objective—The NLRP3 inflammasome plays key roles in inflammation and autoimmunity, and puriner-gic receptor $P2X_7$ has been proposed to be upstream of NLRP3 activation. The aim of the present study, using murine models, was to investigate whether the $P2X_7$/ NLRP3 inflammasome pathway contributes to the pathogenesis of lupus nephritis (LN).

Methods—MRL/*lpr* mice were treated with the selective $P2X_7$ antagonist brilliant blue G (BBG) for 8 weeks. Following treatment, the severity of renal lesions, production of anti-double-stranded DNA (anti-dsDNA) antibodies, rate of survival, activation of the NLRP3/ ASC/caspase 1 inflammasome pathway, and ratio of Thl7 cells to Treg cells were evaluated. $P2X_7$-targeted small interfering RNA (siRNA) was also used for in vivo intervention. Similar evaluations were carried out in NZM2328 mice, a model of LN in which the disease was accelerated by administration of adenovirus-expressing interferon-α (AdIFNα).

Results—Significant up-regulation of $P2X_7$/NLRP3 inflammasome signaling molecules was detected in the kidneys of MLR/*lpr* mice as compared with normal control mice. Blockade of $P2X_7$ activation by BBG suppressed NLRP3/ASC/caspase 1 assembly and the subsequent release of interleukin-1β (IL-1β), resulting in a significant reduction in the severity of nephritis and circulating anti-dsDNA antibodies. The lifespan of the treated mice was significantly prolonged. BBG treatment reduced the serum levels of IL-1β and IL-17 and the Thl7:Treg cell ratio. Similar results were obtained by specific siRNA silencing of $P2X_7$ in vivo. The effectiveness of BBG treatment in modulating LN was confirmed in NZM2328 mice with AdIFNα-accelerated disease.

Address correspondence to Niansheng Yang, MD, PhD, Department of Rheumatology, First Affiliated Hospital, Sun Yat-sen University, 58 Zhongshan Road II, Guangzhou 510080, China, zsuyns@163.com.
Drs. Zhao, Hongyue Wang, and Dai contributed equally to this work.

Author Contributions: All authors were involved in drafting the article or revising it critically for important intellectual content, and all authors approved the final version to be published. Drs. Yang and Fu had full access to all of the data in the study and take responsibility for the integrity of the data and the accuracy of the data analysis.
Study conception and design. Zhao, Hongyue Wang, Dai, Yang, Fu.
Acquisition of data. Zhao, Hongyue Wang, Dai, Hongyang Wang, Zhang, Huang, Shuang Wang, Gaskin, Yang, Fu.
Analysis and interpretation of data. Zhao, Hongyue Wang, Dai, Hongyang Wang, Zhang, Huang, Shuang Wang, Gaskin, Yang, Fu.

Conclusion—Activation of the $P2X_7$ signaling pathway accelerates murine LN by activating the NLRP3/ASC/caspase 1 inflammasome, resulting in increased IL-1β production and enhanced Thl7 cell polarization. Thus, targeting of the $P2X_7$/NLRP3 pathway should be considered as a novel therapeutic strategy in patients with lupus.

The most commonly affected organ in systemic lupus erythematosus (SLE) is the kidney, and lupus nephritis (LN) is a very frequent and potentially fatal complication of SLE (1). Despite the fact that the prognosis has improved over the past few decades, lupus still progresses to end-stage renal disease within 10 years of diagnosis in 10–15% of patients (2). Thus, development of novel therapeutic strategies remains a priority, and to achieve this aim, identification of the specific pathways involved in the modulation of inflammation and autoimmunity is a crucial step.

In addition to the production of various autoantibodies, inflammation is considered to be a key mediator of renal damage in SLE (3). Interleukin-1β (IL-1β) has been recognized as playing several critical roles in the promotion of inflammation in LN (4–6). Levels of IL-1β are increased in the kidneys of lupus-prone mice in 2 classic murine models, and increased IL-1β levels are associated with renal lesions (5,6). Mice lacking IL-1β are resistant to the development of lupus induced by injection of anti-DNA antibodies (7).

NLRP3 (also known as NALP3 or cryopyrin) has recently become the focus of increasing attention in translational research in inflammation. NLRP3 is the best-characterized intracellular receptor, comprising nucleotide-binding oligomerization domain–like and leucine-rich repeat–containing receptors (NLRs). It plays a crucial role in both immunity and inflammation (8). Upon activation, NLRP3 undergoes a conformational change and interacts with an adaptor protein known as ASC, which in turn bridges NRLP3 to procaspase 1 via its caspase activation and recruitment domain, allowing for activation of caspase 1 (8). The resulting multiprotein complex, composed of NLRP3, ASC, and caspase 1 (referred to as the NLRP3 inflammasome), serves as a molecular platform that mediates the autoactivation of caspase 1. Once activated, caspase 1 can cleave the pro forms of IL-1β and IL-18 into then-mature and active forms.

Relevant to the present investigation is the role of NLRP3 in the pathogenesis of LN. Endogenous Ul small nuclear RNP (Ul snRNP) has been shown to activate the NLRP3 inflammasome, suggesting that this pathway might participate in the development of SLE (9). The purinergic receptor $P2X_7$ participates in the processing and release of IL-1β, and has been proposed to be upstream of NLRP3 inflammasome assembly (10). In addition, $P2X_7$ has been reported to be a candidate gene for lupus susceptibility in both murine and human studies (11). In this study, performed in lupus-prone mice, the results demonstrated that $P2X_7$/NLRP3 contributes to the development of LN. Blockade of $P2X_7$ effectively ameliorated LN, via inhibition of formation of the NLRP3 inflammasome.

Materials and Methods

Animals

Female MRL/*lpr* mice were purchased from SLAC Laboratory Animal Company and housed under specific pathogen-free conditions in the Experimental Animal Center at Sun Yat-sen University (Guangzhou, China). Female NZM2328 mice were kept at the Comparative Medicine Center of the University of Virginia School of Medicine (Charlottesville). Experiments were approved by the Ethics Committee of Sun Yat-sen University and the Vertebrate Animal Utilization Committee of the University of Virginia. The mice were kept at these pathogen-free facilities and the experiments were performed in accordance with the National Institutes of Health Guide for Care and Use of Animals. Age-matched female MRL/MpJ mice were used as normal controls.

Brilliant blue G (BBG) treatment

Twelve-week-old MRL/*lpr* mice were randomized into 1 of 2 treatment groups (n = 10 mice per group). BBG (Sigma-Aldrich) was diluted at 3 mg/ml in vehicle (saline) solution. Mice were treated intra-peritoneally with either BBG (45.5 mg/kg) or vehicle every 48 hours, as previously described (12).

Treatment was administered for 8 weeks, and thereafter the mice were anesthetized and killed at age 20 weeks to obtain blood and kidney samples. Both kidneys were perfused to remove the residual blood. A coronal slice of the kidney was fixed in 10% neutral-buffered formalin and then embedded in paraffin. The remaining kidney tissue was snap-frozen in liquid nitrogen and stored at −80°C. Two additional groups of 12-week-old female MRL/*lpr* mice (n = 15 mice per group) were used to calculate the survival rate from 12 weeks to 30 weeks of age.

For experiments with NZM2328 mice, 3-month-old female NZM2328 mice were injected intravenously with 1×10^7 particles of adenovirus-expressing interferon-α (AdIFNα; a kind gift from Dr. Anne Davidson, Feinstein Institute for Medical Research, New York, NY). AdIFNα-injected mice were then treated intraperitoneally with either BBG (45.5 mg/kg) or vehicle every 48 hours. Groups of 4–5 mice were followed up for 3, 4, or 5 weeks. At 5 weeks after AdIFNα injection, the mice were killed.

In vivo small interfering RNA (siRNA) administration

High-dose (0.45 mg/kg) $P2X_7$ siRNA or control siRNA (Santa Cruz Biotechnology) was administered intraperitoneally (n = 6 mice per group) based on previously validated protocols (13,14). Briefly, siPORT amine (Ambion) was incubated in saline for 30 minutes at 22°C. Thereafter, the $P2X_7$ siRNA mixed with an equal volume of siPORT amine, was incubated for 30 minutes at 22°C. The mixture was administered in a total volume of 200 μl. The mice received siRNA every 72 hours, beginning at age 14 weeks (day 0), and thereafter on days 3, 6, and 9. On day 10, the mice were killed, and the efficacy of siRNA silencing was assessed by Western blotting using a mouse anti-$P2X_7$ antibody (Abeam).

Biochemistry

Blood urea nitrogen (BUN) levels were analyzed using a commercial autoanalyzer (Beckman Coulter) at the end of the experiment. Mice were placed in metabolic cages for 24-hour urine collection every 2 weeks, starting when the mice were age 12 weeks. Urinary protein excretion was tested using Multistix 10SG reagent strips (Bayer Healthcare) and graded on a scale of 0–4, where 0 = none, 1 = 30–100 mg/dl, 2 = >100–300 mg/dl, 3 = >300–2,000 mg/dl, and 4 = >2,000 mg/dl (15). For experiments with NZM2328 mice, 24-hour urine samples were collected. The samples were assessed by immunodiffusion for albumin levels and by the picric acid method for creatinine levels.

Evaluation of renal histopathologic features and immune complex deposition

Paraffin-embedded sections of renal tissue were stained with hematoxylin and eosin and periodic acid-Schiff reagents. Histopathologic findings of glomerular and renal vascular lesions were semiquantitatively graded for severity, in a blinded manner, on a scale of 0–3, as reported previously (16).

For detection of immune complex deposition, frozen kidney sections were stained for mouse immunoglobulins and C3 with fluorescein isothiocyanate (FITC)–conjugated rabbit anti-mouse IgG (Santa Cruz Biotechnology), Alexa Fluor 555–conjugated goat anti-mouse IgG (R&D Systems), or FITC-conjugated goat IgG fraction to mouse complement C3 (Cedarlane), after being blocked with 10% fetal bovine serum. The mean intensity of fluorescence was scored 0–3, using previously described methods (17).

Measurement of serum anti–double-stranded DNA (anti-dsDNA) antibodies and cytokines

Serum anti-dsDNA antibodies were measured by enzyme-linked immunosorbent assay (ELISA), as described previously (16). Briefly, 96-well plates were precoated with methylated bovine serum albumin (BSA) at a concentration of 10 mg/ml, followed by 5 μg/ml calf thymus dsDNA (Sigma-Aldrich). After blockade with 1% BSA, serum was added in serial dilutions, starting at 1:40, and incubated at room temperature for 1 hour. A mouse anti-dsDNA monoclonal antibody (Chemicon International) was used to prepare a reference standard curve. After washing, horseradish peroxidase (HRP)–conjugated goat anti-mouse IgG antibody (Sigma-Aldrich) was added to detect the bound anti-dsDNA, followed by a peroxidase substrate, tetramethyl-benzidine. The reaction was terminated with 1M H_2S0_4, and the absorbance at optical density 450 nm (unless indicated otherwise) was determined. The anti-dsDNA levels were quantified with reference to the standard curve. Normal mouse IgG was used as negative control. Levels of IL-1β and IL-17 were assayed using ELISA kits (R&D Systems), according to the manufacturer's instructions.

Western blotting

Kidney tissue was lysed in cell lysis buffer (Cell Signaling Technology) and homogenized, followed by centrifugation at 15,000g. The extracted protein was mixed with 2× sodium dodecyl sulfate (SDS) sample buffer at a 1:1 ratio and boiled. SDS–polyacrylamide gel electrophoresis was conducted with 12.5% gel, and proteins were transferred onto a nitrocellulose membrane. After being blocked with 5% skim milk powder in TBST (Tris

buffered saline with 0.1% Tween 20), the membranes were incubated overnight at 4°C with the following primary antibodies: mouse anti-NLRP3 and anti-$P2X_7$ antibodies (both from Abcam), and anti–caspase l-p20 and anti-GAPDH antibodies (both from Santa Cruz Biotechnology). After washing, blots were incubated with secondary antibodies conjugated to HRP. The signals on the membrane were detected with enhanced chemiluminescence (Cell Signaling Technology).

Isolation of mouse splenocytes

MRL/*lpr* mice were placed under anesthesia and killed by cervical dislocation, and the spleens were removed and dissociated in RPMI medium supplemented with 50 m*M* HEPES and 10% fetal bovine serum. The cell suspension was passed through a 70-μm strainer, and cells were collected by centrifugation at 300g for 5 minutes. Erythrocytes were lysed by incubating the cells in red blood cell lysis buffer (Sigma-Aldrich) at room temperature for 5 minutes. The splenocytes were washed 3 times and collected for flow cytometry analysis.

Flow cytometry

Single-cell suspensions were prepared from the collected splenocytes and incubated with FITC-conjugated anti-mouse CD4, phycoerythrin (PE)–conjugated anti-mouse CD25, PE–Cy5–conjugated anti-mouse FoxP3 (FJK-16s), PE-conjugated anti-mouse IL-17, or their respective isotype controls, for evaluation of T cell subsets. Staining for FoxP3 was conducted using an eBioscience FoxP3 staining kit. Cells were washed and analyzed using FACSCanto system (Becton Dickinson Immunocytometry Systems).

For detection of Thl7 cells, splenocytes (1×10^6 cells/well) were incubated with 50 ng/ml phorbol myristate acetate and 1 μg/ml ionomycin (MultiSciences) in the presence of brefeldin A/monensin mixture (MultiSciences) for 5 hours, before intracellular staining. Analyses were performed using Flow Jo software (Tree Star).

Statistical analysis

Data are expressed as the mean ± SD. Student's *t*-test, one-way analysis of variance, or the nonparametric Wilcoxon rank-sum test were used for data analysis. The Kaplan-Meier method and log-rank analysis were used to compare mouse survival rates. All data were analyzed using SPSS software (version 16.0). *P* values less than 0.05 were considered significant.

Results

Inhibitory effects of BBG on activation of the NLRP3 inflammasome in MRL/*lpr* mice

Renal expression of the $P2X_7$/NLRP3 inflammasome pathway was examined in 20-week-old MRL/*lpr* mice and in age-matched MRL/MpJ mice as normal controls (n = 6 mice per group). Enhanced protein expression of $P2X_7$, NLRP3, and ASC was observed in the kidneys from MRL/*lpr* mice compared with the kidneys from normal control mice (Figure 1A). The active caspase l-p20 subunit represents the highly active p20/pl0 tetrameric forms of processed caspase 1. Expression of the p20 subunit of caspase 1 was significantly elevated in the kidneys from MRL/*lpr* mice compared with the kidneys from normal control

mice ($P < 0.01$). In addition, levels of IL-1β in the kidney homogenates were significantly increased in MRL/*lpr* mice compared with normal control mice ($P < 0.01$) (Figure 1C).

The effects of the selective $P2X_7$ inhibitor BBG on activation of the NLRP3 inflammasome in MRL/*lpr* mice were tested. Western blot analysis showed that 8 weeks of treatment with BBG resulted in suppressed renal expression of NLRP3, ASC, and caspase l-p20 (Figure 1B). Furthermore, renal and serum levels of IL-1β were significantly reduced after BBG treatment ($P < 0.01$) (Figures 1D and E).

Reduction in renal damage following BBG treatment in MRL/*lpr* mice

To assess the effects of the $P2X_7$ inhibitor BBG on renal function, we measured 24-hour urinary protein excretion every 2 weeks, starting at week 12 up to week 20. Both the BBG-treated group and the vehicle-treated control group displayed a progressive increase in proteinuria over time, starting from week 12 (Figure 2A), but the trend was reversed at 18 weeks in BBG-treated mice. As compared with vehicle-treated mice, proteinuria was significantly reduced by BBG treatment at week 18 ($P < 0.05$) and at week 20 ($P < 0.01$). In addition, BUN levels at the end of treatment were significantly lower in the BBG-treated group compared with the vehicle-treated group ($P < 0.05$) (Figure 2B).

Pathologic features of the kidney were also compared between vehicle-treated and BBG-treated MRL/ *lpr* mice at 20 weeks. The kidneys of mice surviving to 20 weeks of age were collected for histopathologic analysis. The analysis revealed that vehicle-treated mice exhibited the typical features of renal disease, with diffuse glomerulonephritis (enlarged hypercellular glomeruli, crescent formation) and perivascular lesions (vasculitis). In contrast, BBG-treated mice showed significantly diminished glomerular hypercellularity, crescent formation, and perivascular lesions (vasculitis) (Figures 2C and D).

Reduction in renal immune complex deposition, serum anti-dsDNA production, and mortality following BBG treatment in MRL/*lpr* mice

To determine whether $P2X_7$ inhibition might affect renal disease by reducing immune complex deposition in the kidneys, kidney sections were stained for C3 and IgG. No immune complex was observed in normal control samples. However, intense deposition of C3 and IgG was detected in the glomeruli of vehicle-treated mice (Figure 2E). As expected, semiquantitative scoring of the fluorescence intensity by digital imaging microscopy showed that BBG treatment led to a remarkable decrease in glomerular deposition of C3 and IgG ($P < 0.01$) (Figure 2F).

Furthermore, the circulating anti-dsDNA antibody levels, as determined by ELISA, were significantly different between the vehicle-treated control group and the BBG-treated group at week 20 ($P < 0.01$) (Figure 3A). These results indicate that BBG treatment suppressed the production of anti-dsDNA antibodies in MRL/*lpr* mice. In contrast, no serum anti-dsDNA antibody was detected in normal control mice.

To examine the impact of $P2X_7$ inhibition on lifespan, 2 groups of MRL/*lpr* mice, treated with either vehicle or BBG, were followed up until the emergence of multiple signs of impending death (i.e., decreased activity, lowered body temperature, and weight loss), as

judged by 2 observers. The mice were then killed at age 30 weeks. We observed a significant survival benefit in mice treated with BBG as compared with vehicle-treated control mice ($P < 0.05$) (Figure 3B).

Reduction in Thl7:Treg cell ratio by BBG treatment

The Thl7:Treg cell ratio in the spleens of BBG-treated and vehicle-treated MRL/*lpr* mice was determined by flow cytometry analysis. As shown in Figure 3C, a diminution in Thl7 cells and an increase in Treg cells were observed in mice treated with BBG for 8 weeks, resulting in a pronounced reduction in the Thl7: Treg cell ratio (Figure 3D).

Consistent with these results, BBG treatment also resulted in a prominent decrease in the serum IL-17 levels in MRL/*lpr* mice (Figure 3E). These results suggest that the $P2X_7$ pathway may contribute to the Thl7:Treg cell imbalance.

$P2X_7$ siRNA modulation of autoimmunity and cytokine production in MRL/*lpr* mice

$P2X_7$ siRNA was administered to MRL/*lpr* mice, as described previously in studies by Natarajan et al (13) and Mezzaroma et al (14). Treatment with siRNA was started in the mice at age 14 weeks, given once every 72 hours and continued for 10 days. $P2X_7$ siRNA treatment reduced the expression of $P2X_7$ protein in the mouse kidneys by more than 85% and the expression of NLRP3 by more than 50% (Figure 4A). Anti-dsDNA antibody production in MRL/*lpr* mice was also significantly inhibited by $P2X_7$ siRNA treatment as compared with control siRNA treatment (Figure 4B). The ratio of Thl7 cells to Treg cells in the splenocytes was strikingly decreased in MRL/*lpr* mice treated with $P2X_7$ siRNA (Figure 4C). Moreover, $P2X_7$ siRNA–treated mice produced lower serum levels of IL-1β and IL-17 when compared with control siRNA– treated mice (Figures 4D and E).

Modulation of disease in BBG-treated NZM2328 mice with AdIFNα-accelerated LN

Although MRL/*lpr* mice have been used in experimental models of human LN, the disease in these mice is primarily driven by inflammation resulting from Fas deficiency. The effectiveness of BBG on LN was tested in NZM2328 mice, a model in which the disease resembles immune complex-mediated proliferative glomerulonephritis (18), and ~70% of female NZM2328 mice develop chronic glomerulonephritis by the age of 12 months. In order to shorten the duration of the experiments, AdIFNα was administered to 3-month-old female NZM2328 mice. Mice injected with AdIFNα develop accelerated glomerulonephritis, in conjunction with severe proteinuria, within 4–5 weeks after the administration of the virus, similar to the accelerated glomerulonephritis seen in similarly treated (NZB × NZW)F_1 mice (19,20).

In a preliminary experiment with BBG-treated and vehicle-treated NZM2328 mice (n = 5 per group), treatment with BBG was effective in delaying the onset of proteinuria. A second experiment was carried out with 5 mice in each group. The combined data from these 2 experiments are shown in Figure 5A. By 30 days after the administration of AdIFNα, 7 of 10 mice in the group that was treated with vehicle developed severe proteinuria (>300 mg/ml albuminuria), whereas only 1 of the 10 mice in the BBG-treated group developed severe proteinuria.

Blood and 24-hour urine samples were collected from the mice in the second experiment, prior to termination of the experiment at the end of 5 weeks after AdIFNα administration. As shown in Figures 5B–F, treatment of the mice with BBG significantly reduced the urinary albumi:creatinine ratio, serum BUN levels, serum anti-dsDNA antibody levels, and serum and renal IL-1β levels. Morphologically, BBG-treated mice had relatively normal renal histologic features (Figures 6A and C) and reduced staining for C3 and IgG deposits (Figures 6B and D).

Discussion

$P2X_7$ is an extracellular ATP-gated plasma membrane ion channel receptor that has multiple biologic functions and is expressed on a wide variety of immune cells (21). In addition, $P2X_7$ has been shown to act as a proinflammatory trigger (10). $P2X_7$ is significantly up-regulated in response to inflammatory stimuli, and activation of this receptor initiates and amplifies the innate immune response and IL-lβ–centered proinflammatory cascades (21,22). Activation of the $P2X_7$ receptor contributes to autoimmune inflammation of the salivary gland in patients with Sjögren's syndrome (23).

Furthermore, $P2X_7$ antagonism was shown to ameliorate experimental autoimmune encephalomyelitis (EAE) in mice (24) and has been detected at very low levels in normal rat and mouse kidneys, but is significantly up-regulated in renal inflammation (25). Of note, results of gene mapping suggest that murine and human $P2X_7$ lies within a lupus susceptibility locus (11). $P2X_7$ expression has also been shown to be up-regulated in renal biopsy tissue from patients with lupus (26). However, the functional roles of $P2X_7$ have not been studied in patients with SLE.

In this study, we found that there was significant up-regulation of $P2X_7$ expression at the protein level in the kidneys of MRL/*lpr* mice, in close association with increased IL-1β production and renal damage. Strikingly, blockade of the $P2X_7$ signaling pathway prevented the development of LN, and also resulted in a reduction in proteinuria and BUN levels. In addition, BBG-treated mice displayed a prolonged lifespan. In view of recent findings suggesting that BBG may have other pharmacologic effects in addition to its inhibitory effects on the $P2X_7$ receptor (27), we performed additional experiments with $P2X_7$ siRNA. Short-term treatment with $P2X_7$ siRNA had effects on MRL/*lpr* mice that were similar to those of BBG. It inhibited $P2X_7$/NLRP3 activation, reduced the production of IL-1β and IL-17, decreased the Thl7:Treg cell ratio, and decreased the levels of circulating anti-dsDNA antibodies. Thus, the results of this study indicate that $P2X_7$ may be a target for therapy in SLE.

Although there are exceptions (28), the central role of $P2X_7$ in the release of mature IL-1β and IL-18 is now well established (21,22). The critical link between $P2X_7$, mature IL-1β, and NLRP3 has not been uncovered until recently. $P2X_7$ has been demonstrated to be a potent activator of the NLRP3 inflammasome (29). Assembly of the NLRP3/ASC/caspase 1 complex facilitates caspase 1–mediated processing and release of the proinflammatory cytokines IL-1β and IL-18 (8). Previous studies have revealed that Ul snRNP is a potential signal that activates the NLRP3 inflammasome in autoimmune diseases such as SLE (9),

while an increase in IL-18 production, which is induced by activation of the NLRP3 inflammasome, will result in endothelial progenitor cell dysfunction in SLE (30), suggesting that NLRP3 has a pathogenic role in this disease. Our results indicated that NLRP3 was activated in the kidneys of MKL/*lpr* mice, in conjunction with enhanced expression of $P2X_7$. Blockade of $P2X_7$ was associated with inhibition of NLRP3 activation, suppression of IL-1β production, and attenuation of renal damage, indicating that the $P2X_7$/NLRP3 pathway is involved in the pathogenesis of LN.

In addition to NLRP3, the role of ASC in the assembly of the inflammasome complex has been elucidated in a number of studies (8,30–33). ASC functions as an adaptor protein by linking NLRP3 and procaspase 1, thereby activating caspase 1 to produce the inflammatory cytokines IL-1β and IL-18 (8). Recent studies have shown that ASC contributes greatly to the pathogenesis of autoimmune diseases, such as EAE and collagen-induced arthritis (31,32). In this regard, it is of interest to note that the expression of ASC in peripheral lymphocytes and renal biopsy tissue from SLE patients was significantly elevated (30,33). In this study, the protein level of ASC was significantly up-regulated in the kidneys of MRL/*lpr* mice. Strikingly, blockade of $P2X_7$ suppressed the expression of this inflammasome component, and also suppressed the production of IL-1β, suggesting that the therapeutic effects of $P2X_7$ blockade are mediated via the NLRP3/ASC/caspase 1 complex.

Notably, IL-1β plays a critical role in the regulation of the Thl7:Treg cell balance. Studies in vitro and in vivo have indicated that, under neutral conditions, simultaneous activation of Treg cells and naive CD4+ T cells in the presence of antigen-presenting cells will lead to conversion of Treg cells into Thl7 cells, and endogenous IL-1β is necessary in this process (34). IL-1β has also been shown to reduce the function of Treg cells and promote their conversion into Thl7 cells (35). Consistent with these findings, the present study demonstrated that inhibition of $P2X_7$ diminished the percentage of Thl7 cells and increased the percentage of Treg cells, resulting in a decreased Thl7:Treg cell ratio.

Of note, the Thl7:Treg cell imbalance is closely involved in the pathogenesis of SLE. One study showed that decreased numbers of Thl7 cells were associated with attenuated LN (36). Moreover, increased production of IL-17 contributed critically to the development of lethal pathologic features in a mouse model of lupus (37). In contrast, expansion of Treg cells was protective against chronic graft-versus-host disease–induced LN in mice (38). Animal studies have shown that a reduction in Treg cells and expansion of Thl7 cells were positively associated with the presence of T cell infiltrates that promoted severe nephritis (39). In human SLE, Thl7 cells have been shown to infiltrate the kidneys and cause renal damage by up-regulating the expression of inflammatory cytokines and chemokines (40,41). In the present study, inhibition of $P2X_7$ reduced the Thl7:Treg cell ratio, and this effect is most likely mediated, in part, by inhibition of the generation of IL-1β. It remains to be determined whether BBG has a direct effect on T cell homeostasis. Nevertheless, the results of this study suggest that IL-1 may be a target for therapy in LN. This conclusion is further supported by the findings of a preliminary clinical trial showing that anakinra (IL-1 receptor antagonist) is effective in treating SLE patients with severe arthritis (42).

Moreover, the results of our study showed that $P2X_7$ inhibition resulted in a significant decrease in the production of autoantibodies and immune complex deposition in the mouse kidneys. The mechanism of action of $P2X_7$ inhibition with regard to its effects on autoantibody production remains to be clarified. However, it may be associated with the reduced number of Thl7 cells following $P2X_7$ blockade. Thl7 cells have been shown to function as B cell helpers, both in vitro and in vivo, which favors the activation of autoreactive B cells and the production of pathogenic antibodies (43). Thl7 cells also directly promote B cell activation and differentiation into antibody-producing cells in the target organs (43,44). These findings are consistent with those in a study showing that decreased numbers of Thl7 cells were accompanied by a reduction in circulating anti-dsDNA antibodies in C5TBL/6-*lpr/lpr* mice (36). Alternatively, since $P2X_7$ is also expressed on B cells (43), blockade of $P2X_7$ might also have a direct effect on autoantibody-producing B cells.

The effectiveness of BBG in modulating lupuslike glomerulonephritis was also shown in AdlFNα-infected NZM2328 mice. BBG effectively blocked the development of autoantibodies, severe proteinuria, and immune complex-mediated glomerulonephritis. In this model, IL-1β production was reduced significantly in the serum and renal tissue. The results of these experiments in NZM2328 mice suggest that blocking the $P2X_7$ pathway to interfere with the development of LN may have more general applicability in the treatment of LN.

Taken together, the results of this study identify a new target for LN therapy. Our data have shown that inhibition of $P2X_7$ signaling effectively ameliorated LN by inhibiting NLRP3 inflammasome activation. Therefore, development of pharmacologic inhibitors targeting the $P2X_7$/NLRP3 signaling pathway would be helpful in providing novel therapeutic strategies for human SLE. In view of the complexity of the pathogenesis of LN, targeting of the $P2X_7$/NLRP3 pathway should be a part of the multitarget approach in this disease.

Acknowledgments

Supported by the National Natural Science Foundation of China (grant 81273278), the Ministry of Education of China (PhD Program Foundation grant 20120171110064), the Guangdong Natural Science Foundation (grants S2012010008780 and S2011010004578), the Guangzhou Science and Technology Planning Program (grant 2012J4100085), and the Sun Yat-sen Innovative Talents Cultivation Program for Doctoral Graduate Students. Dr. Fu's work was supported in part by National Institute of Arthritis and Musculoskeletal and Skin Diseases grants (R01-AR047988 and R01-AR049449) and a grant from the Alliance for Lupus Research.

References

1. Cameron JS. Lupus nephritis. J Am Soc Nephrol. 1999; 10:413–24. [PubMed: 10215343]
2. Faurschou M, Dreyer L, Kamper AL, Starklint H, Jacobsen S. Long-term mortality and renal outcome in a cohort of 100 patients with lupus nephritis. Arthritis Care Res (Hoboken). 2010; 62:873–80. [PubMed: 20191478]
3. Munoz LE, Janko C, Grossmayer GE, Frey B, Voll RE, Kern P, et al. Remnants of secondarily necrotic cells fuel inflammation in systemic lupus erythematosus. Arthritis Rheum. 2009; 60:1733–42. [PubMed: 19479824]
4. Dinarello CA. Interleukin-1 in the pathogenesis and treatment of inflammatory diseases. Blood. 2011; 117:3720–32. [PubMed: 21304099]

5. Boswell JM, Yui MA, Burt DW, Kelley VE. Increased tumor necrosis factor and IL-1β gene expression in the kidneys of mice with lupus nephritis. J Immunol. 1988; 141:3050–4. [PubMed: 3262676]
6. Brennan DC, Yui MA, Wuthrich RP, Kelley VE. Tumor necrosis factor and IL-1 in New Zealand black/white mice: enhanced gene expression and acceleration of renal injury. J Immunol. 1989; 143:3470–5. [PubMed: 2584702]
7. Voronov E, Dayan M, Zinger H, Gayvoronsky L, Lin JP, Iwakura Y, et al. IL-lβ-deficient mice are resistant to induction of experimental SLE. Eur Cytokine Netw. 2006; 17:109–16. [PubMed: 16840029]
8. Saleh M. The machinery of Nod-like receptors: refining the paths to immunity and cell death. Immunol Rev. 2011; 243:235–46. [PubMed: 21884180]
9. Shin MS, Kang Y, Lee N, Kim SH, Kang KS, Lazova R, et al. Ul-small nuclear ribonucleoprotein activates the NLRP3 inflam-masome in human monocytes. J Immunol. 2012; 188:4769–75. [PubMed: 22490866]
10. Ferrari D, Pizzirani C, Adinolfi E, Lemoli RM, Curti A, Idzko M, et al. The P2X7 receptor: a key player in IL-1 processing and release. J Immunol. 2006; 176:3877–83. [PubMed: 16547218]
11. Elliott JI, McVey JH, Higgins CF. The P2X7 receptor is a candidate product of murine and human lupus susceptibility loci: a hypothesis and comparison of murine allelic products. Arthritis Res Ther. 2005; 7:R468–75. [PubMed: 15899033]
12. Diaz-Hernandez M, Diez-Zaera M, Sanchez-Nogueiro J, Gomez-Villafuertes R, Canals JM, Alberch J, et al. Altered P2X7-receptor level and function in mouse models of Huntington's disease and therapeutic efficacy of antagonist administration. FASEB J. 2009; 23:1893–906. [PubMed: 19171786]
13. Natarajan R, Salloum FN, Fisher BJ, Kukreja RC, Fowler AA III. Hypoxia inducible factor-1 activation by prolyl 4-hydroxylase-2 gene silencing attenuates myocardial ischemia reperfusion injury. Circ Res. 2006; 98:133–40. [PubMed: 16306444]
14. Mezzaroma E, Toldo S, Farkas D, Seropian IM, Van Tassell BW, Salloum FN, et al. The inflammasome promotes adverse cardiac remodeling following acute myocardial infarction in the mouse. Proc Natl Acad Sci U S A. 2011; 108:19725–30. [PubMed: 22106299]
15. Jiang C, Foley J, Clayton N, Kissling G, Jokinen M, Herbert R, et al. Abrogation of lupus nephritis in activation-induced deaminase-deficient MRL/lpr mice. J Immunol. 2007; 178:7422–31. [PubMed: 17513793]
16. Muraoka M, Hasegawa H, Kohno M, Inoue A, Miyazaki T, Terada M, et al. IK cytokine ameliorates the progression of lupus nephritis in MRL/lpr mice. Arthritis Rheum. 2006; 54:3591–600. [PubMed: 17075801]
17. Zhang L, Yang N, Wang S, Huang B, Li F, Tan H, et al. Adenosine 2A receptor is protective against renal injury in MRL/lpr mice. Lupus. 2011; 20:667–77. [PubMed: 21183557]
18. Waters ST, Fu SM, Gaskin F, Deshmukh US, Sung SS, Kannapell CC, et al. NZM2328: a new mouse model of systemic lupus erythematosus with unique genetic susceptibility loci. Clin Immunol. 2001; 100:372–83. [PubMed: 11513551]
19. Mathian A, Winberg A, Gallegos M, Banchereau J, Koutouzov S. IFN-α induces early lethal lupus in preautoimmune (New Zealand Black × New Zealand White)F_1 but not in BALB/c mice. J Immunol. 2005; 174:2499–506. [PubMed: 15728455]
20. Liu Z, Bethunaickan R, Huang W, Lodhi U, Solano I, Madaio MP, et al. Interferon-α accelerates murine systemic lupus erythematosus in a T cell–dependent manner. Arthritis Rheum. 2011; 63:219–29. [PubMed: 20954185]
21. Ferrari D, Pizzirani C, Adinolfi E, Lemoli RM, Curti A, Idzko M, et al. The $P2X_7$ receptor: a key player in IL-1 processing and release. J Immunol. 2006; 176:3877–83. published erratum appears in J Immunol 2007;179:8569. [PubMed: 16547218]
22. North RA. Molecular physiology of P2X receptors. Physiol Rev. 2002; 82:1013–67. [PubMed: 12270951]
23. Woods LT, Camden JM, Batek JM, Petris MJ, Erb L, Weisman GA. P2X7 receptor activation induces inflammatory responses in salivary gland epithelium. Am J Physiol Cell Physiol. 2012; 303:C790–801. [PubMed: 22875784]

24. Matute C, Torre I, Perez-Cerda F, Perez-Samartin A, Alberdi E, Etxebarria E, et al. $P2X_7$ receptor blockade prevents ATP excitotoxicity in oligodendrocytes and ameliorates experimental autoimmune encephalomyelitis. J Neurosci. 2007; 27:9525–33. [PubMed: 17728465]
25. Harada H, Chan CM, Loesch A, Unwin R, Burnstock G. Induction of proliferation and apoptotic cell death via P2Y and P2X receptors, respectively, in rat glomerular mesangial cells. Kidney Int. 2000; 57:949–58. [PubMed: 10720948]
26. Turner CM, Tam FW, Lai PC, Tarzi RM, Burnstock G, Pusey CD, et al. Increased expression of the pro-apoptotic ATP-sensitive $P2X_7$ receptor in experimental and human glomerulonephritis. Nephrol Dial Transplant. 2007; 22:386–95. [PubMed: 17040997]
27. Jo S, Bean BP. Inhibition of neuronal voltage-gated sodium channels by brilliant blue G. Mol Pharmacol. 2011; 80:247–57. [PubMed: 21536754]
28. He Y, Franchi L, Nunez G. TLR agonists stimulate Nlrp3-dependent IL-1β production independently of the purinergic P2X7 receptor in dendritic cells and in vivo. J Immunol. 2013; 190:334–9. [PubMed: 23225887]
29. Di Virgilio F. Liaisons dangereuses: $P2X_7$ and the inflammasome. Trends Pharmacol Sci. 2007; 28:465–72. [PubMed: 17692395]
30. Kahlenberg JM, Thacker SG, Berthier CC, Cohen CD, Kretzler M, Kaplan MJ. Inflammasome activation of IL-18 results in endothelial progenitor cell dysfunction in systemic lupus erythematosus. J Immunol. 2011; 187:6143–56. [PubMed: 22058412]
31. Shaw PJ, Lukens JR, Burns S, Chi H, McGargill MA, Kanneganti TD. Critical role for PYCARD/ASC in the development of experimental autoimmune encephalomyelitis. J Immunol. 2010; 184:4610–4. [PubMed: 20368281]
32. Ippagunta SK, Brand DD, Luo J, Boyd KL, Calabrese C, Stienstra R, et al. Inflammasome-independent role of apoptosis-associated speck-like protein containing a CARD (ASC) in T cell priming is critical for collagen-induced arthritis. J Biol Chem. 2010; 285:12454–62. [PubMed: 20177071]
33. Eggleton P, Harries LW, Alberigo G, Wordsworth P, Viner N, Haigh R, et al. Changes in apoptotic gene expression in lymphocytes from rheumatoid arthritis and systemic lupus erythematosus patients compared with healthy lymphocytes. J Clin Immunol. 2010; 30:649–58. [PubMed: 20532967]
34. Li L, Kim J, Boussiotis VA. IL-lβ-mediated signals preferentially drive conversion of regulatory T cells but not conventional T cells into IL-17-producing cells. J Immunol. 2010; 185:4148–53. [PubMed: 20817874]
35. Bertin-Maghit S, Pang D, O'Sullivan B, Best S, Duggan E, Paul S, et al. Interleukin-1β produced in response to islet autoantigen presentation differentiates T-helper 17 cells at the expense of regulatory T-cells: implications for the timing of tolerizing immunotherapy. Diabetes. 2011; 60:248–57. [PubMed: 20980463]
36. Kyttaris VC, Zhang Z, Kuchroo VK, Oukka M, Tsokos GC. IL-23 receptor deficiency prevents the development of lupus nephritis in C57BL/6-lpr/lpr mice. J Immunol. 2010; 184:4605–9. [PubMed: 20308633]
37. Pisitkun P, Ha HL, Wang H, Claudio E, Tivy CC, Zhou H, et al. Interleukin-17 cytokines are critical in development of fatal lupus glomerulonephritis. Immunity. 2012; 37:1104–15. [PubMed: 23123062]
38. Zhang JL, Sun DJ, Hou CM, Wei YL, Li XY, Yu ZY, et al. CD3 mAb treatment ameliorated the severity of the cGVHD-induced lupus nephritis in mice by up-regulation of $Foxp3^+$ regulatory T cells in the target tissue: kidney. Transpl Immunol. 2010; 24:17–25. [PubMed: 20850528]
39. Xu Z, Cuda CM, Croker BP, Morel L. The NZM2410-derived lupus susceptibility locus Sle2cl increases Thl7 polarization and induces nephritis in fas-deficient mice. Arthritis Rheum. 2011; 63:764–74. [PubMed: 21360506]
40. Wang Y, Ito S, Chino Y, Goto D, Matsumoto I, Murata H, et al. Laser microdissection-based analysis of cytokine balance in the kidneys of patients with lupus nephritis. Clin Exp Immunol. 2010; 159:1–10. [PubMed: 19807734]
41. Ambrosi A, Espinosa A, Wahren-Herlenius M. IL-17: a new actor in IFN-driven systemic autoimmune diseases. Eur J Immunol. 2012; 42:2274–84. [PubMed: 22949326]

42. Ostendorf B, Iking-Konert C, Kurz K, Jung G, Sander O, Schneider M. Preliminary results of safety and efficacy of the interleukin 1 receptor antagonist anakinra in patients with severe lupus arthritis. Ann Rheum Dis. 2005; 64:630–3. [PubMed: 15345502]

43. Lee DH, Park KS, Kong ID, Kim JW, Han BG. Expression of P2 receptors in human B cells and Epstein-Barr virus-transformed lymphoblastoid cell lines. BMC Immunol. 2006; 7:22. [PubMed: 16970829]

44. Mitsdoerffer M, Lee Y, Jager A, Kim HJ, Korn T, Kolls JK, et al. Proinflammatory T helper type 17 cells are effective B-cell helpers. Proc Natl Acad Sci U S A. 2010; 107:14292–7. [PubMed: 20660725]

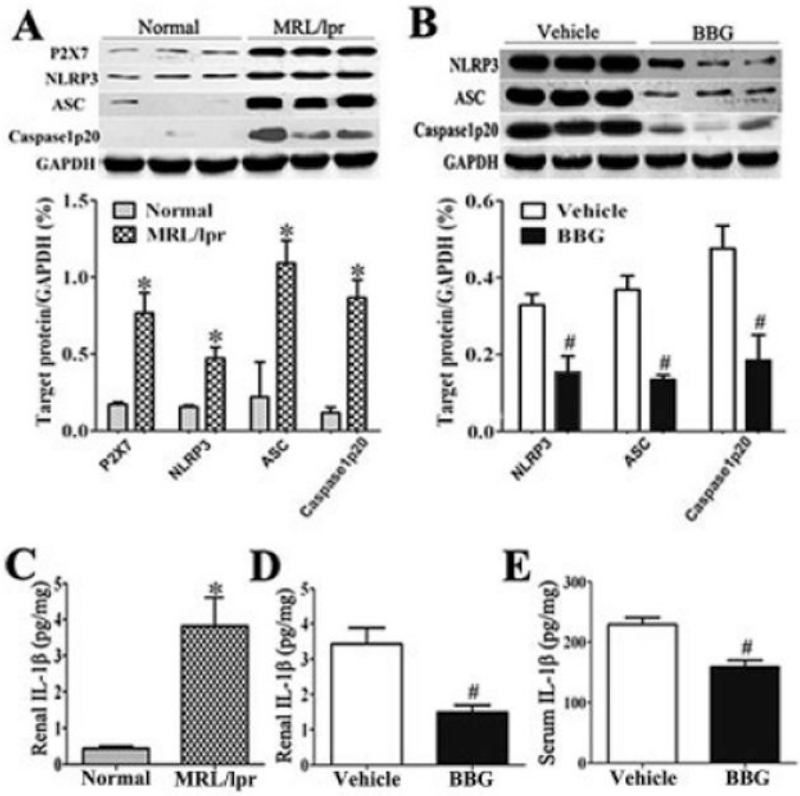

Figure 1.

Treatment of MRL/*lpr* mice with brilliant blue G (BBG) suppresses the activation of the $P2X_7$/NLRP3 pathway. **A** and **B**, Representative Western blot bands (top) and relative expression levels in each group (bottom) show the protein expression of $P2X_7$, NLRP3, ASC, and caspase l-p20, normalized to the values for GAPDH, in the kidneys of 20-week-old MKL/*lpr* mice versus normal controls (age-matched normal MRL/MpJ mice) (n = 6 per group) **(A)**, and the kidneys of BBG-treated MRL/*lpr* mice versus vehicle-treated controls (after 8 weeks of treatment; n = 10 per group) **(B)**. **C–E**, Levels of interleukin-lβ (IL-lβ) were determined by enzyme-linked immunosorbent assay in the kidneys of MRL/*lpr* mice versus normal controls **(C)**, and the kidneys **(D)** and serum **(E)** of BBG-treated MRL/*lpr* mice versus vehicle-treated controls. Results are the mean ± SD. * = $P < 0.01$ versus normal controls; # = $P < 0.01$ versus vehicle-treated controls.

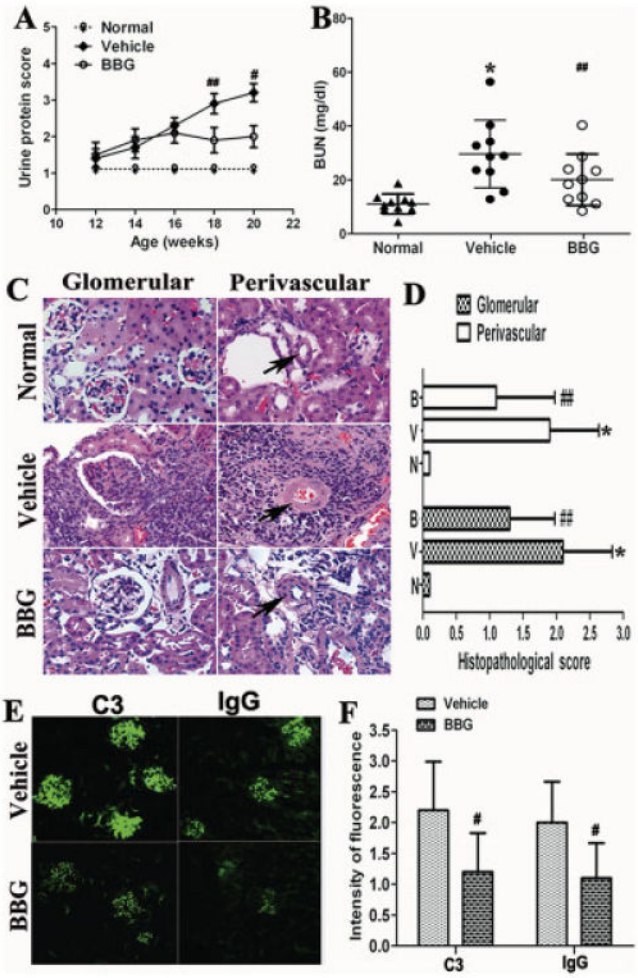

Figure 2.

Treatment of MRL/*lpr* mice with brilliant blue G (BBG) reduces renal lesions and immune complex deposition. **A** and **B**, The 24-hour urinary protein excretion levels (recorded biweekly) **(A)** and blood urea nitrogen (BUN) levels (measured at the end of the experiment) **(B)** were determined in BBG-treated MRL/*lpr* mice versus normal controls (age-matched female MRL/MpJ mice) and vehicle-treated controls. Bars in **B** show the mean ± SD. **C** and **D**, Renal tissue was obtained from 20-week-old MRL/*lpr* mice treated with either BBG or vehicle and from normal control mice for histopathologic analyses. Glomerular and perivascular areas of the renal sections were stained with hematoxylin and eosin to assess features of glomerulonephritis and perivascular lesions (**arrows**) (representative images shown) **(C)**. Original magnification × 400. The severity of renal damage was semiquantitatively scored in each group (B = BBG-treated; V = vehicle-treated controls; N = normal controls) **(D)**. **E** and **F**, Renal sections from BBG-treated and vehicle-treated control mice were snap-frozen and embedded in OCT. The tissue was then analyzed by immunofluorescence microscopy to assess the deposition of C3 and IgG (representative images shown) **(E)** and the intensity of green fluorescence **(F)** after 8 weeks of BBG treatment in comparison with vehicle treatment. Original magnification × 200. Results are

the mean ± SD (n = 10 per group). * = $P < 0.01$ versus normal controls; # = $P < 0.01$ and ## = $P < 0.05$ versus vehicle-treated controls.

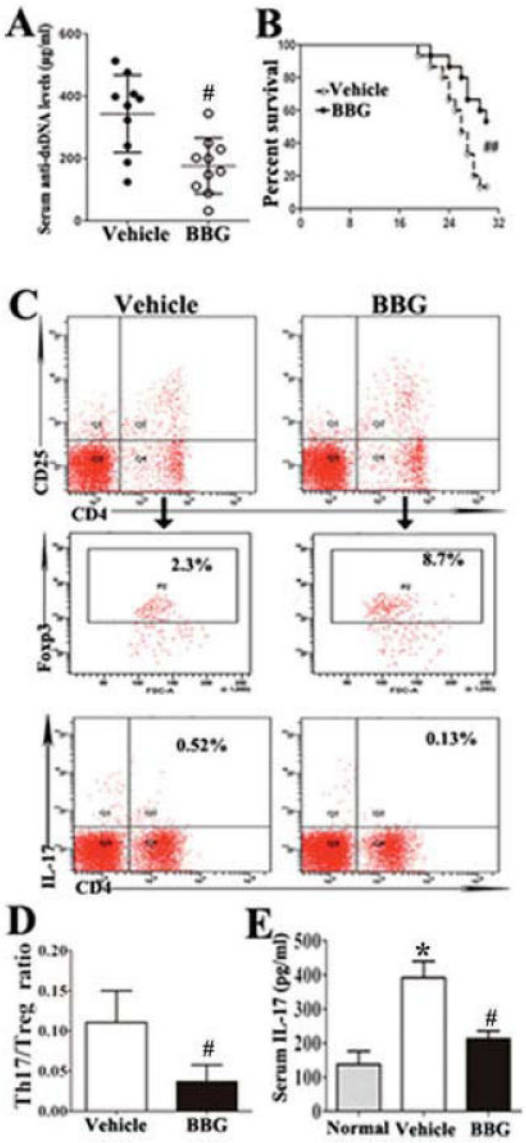

Figure 3.

Treatment of MRL/*lpr* mice with brilliant blue G (BBG) results in reductions in autoantibody production, mortality, and the Thl7:Treg cell ratio. **A** and **B**, Serum anti–double-stranded DNA (anti-dsDNA) antibody levels (n = 10 per group) **(A)** and lifespan (n = 15 per group) **(B)** were compared between BBG-treated MRL/*lpr* mice and vehicle-treated controls. Mice were killed at age 30 weeks. Bars in **A** show the mean ± SD. **C** and **D**, Flow cytometry analyses were used to assess the expression of Treg cells (CD4+CD25+FoxP3+) and Thl7 cells (CD4+IL-17+) in splenocytes of vehicle-treated and BBG-treated MRL/*lpr* mice (representative results shown) **(C)**, and the ratio of Thl7 cells to Treg cells was determined (n = 6 per group) **(D)**. **E**, Serum interleukin-17 (IL-17) levels were compared between the normal control mice and the MRL/*lpr* mice treated with either vehicle or BBG (n = 10 per group). Results are the mean ± SD. * = $P < 0.01$ versus normal controls; # = $P < 0.01$ and ## = $P < 0.05$ versus vehicle-treated controls.

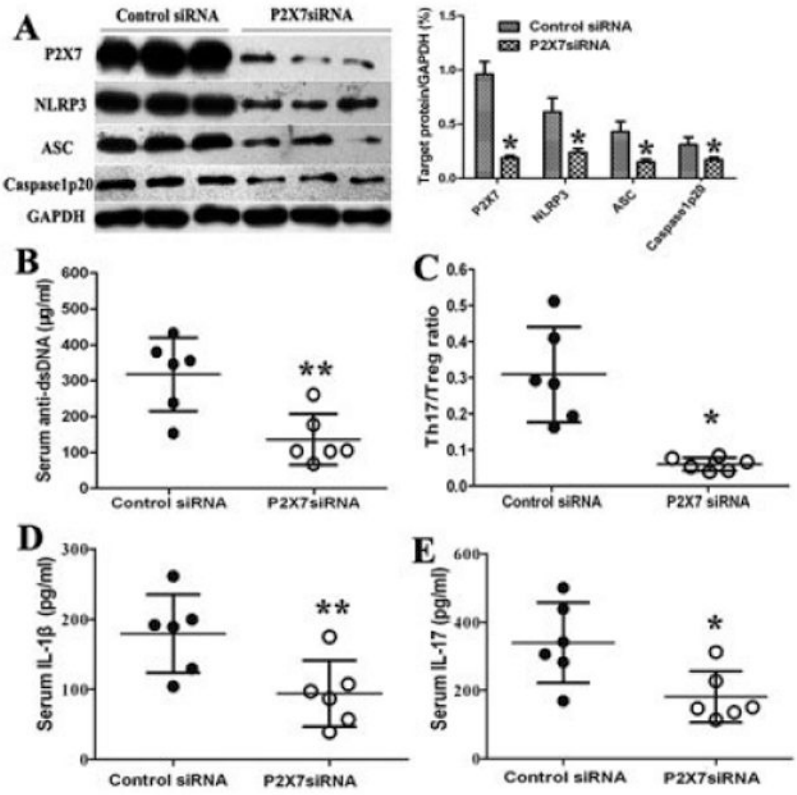

Figure 4.

Effects of $P2X_7$ small interfering RNA (siRNA) treatment on lupus syndrome in MRL/*lpr* mice. MRL/*lpr* mice, age 14 weeks, were treated with either control siRNA or $P2X_7$ siRNA for 10 days. **A**, The kidneys were analyzed by Western blotting (representative bands shown) (left) for relative protein expression of $P2X_7$, NLRP3, ASC, and caspase l-p20, and the results, normalized to the values for GAPDH, were quantified and expressed as the mean ± SD (n = 6 per group) (right). **B–E**, Serum anti–double-stranded DNA (anti-dsDNA) antibody levels (determined by enzyme-linked immunosorbent assay [ELISA]) **(B)**, the Thl7:Treg cell ratio in the spleens **(C)**, serum interleukin-1β (IL-1β) levels (determined by ELISA) **(D)**, and serum IL-17 levels (determined by ELISA) **(E)** were compared between the 2 groups. Bars show the mean ± SD (n = 6 per group). * = $P < 0.01$; ** = $P < 0.05$ versus control siRNA-treated mice.

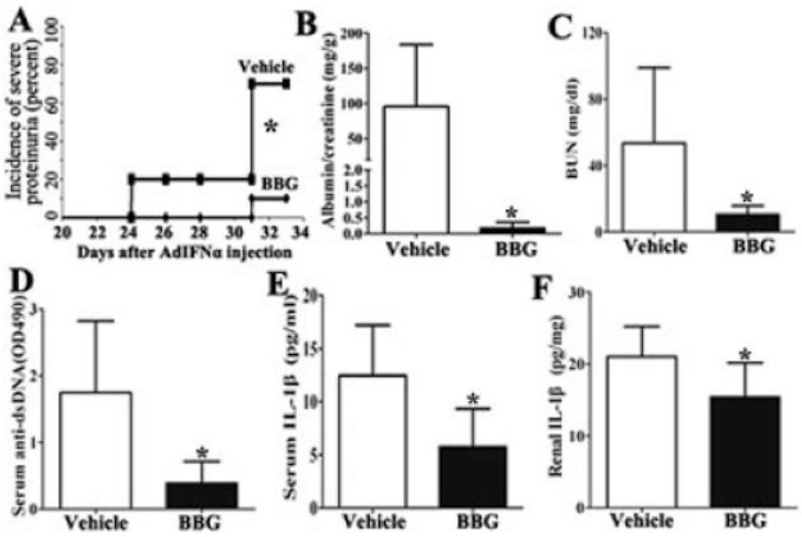

Figure 5.

Treatment of NZM2328 mice with brilliant blue G (BBG) protects kidney function in a model of adenovirus-expressing interferon-α (AdIFNα)-accelerated glomerulonephritis. **A**, Incidence of severe proteinuria was compared between vehicle-treated and BBG-treated mice (n = 10 per group) using Multistix 10SG reagent strips. A protein concentration of ≥300 mg/dl was considered to be severe proteinuria. **B–F**, Albumin and creatinine concentrations (using 24-hour urinary protein samples collected on day 28) **(B)**, blood urea nitrogen (BUN) levels (measured on day 28) **(C)**, anti–double-stranded DNA (anti-dsDNA) antibody levels (determined by enzyme-linked immunosorbent assay) **(D)**, and serum **(E)** and renal **(F)** interleukin-1β (IL-1β) levels (measured at the end of experiment) were compared between the 2 groups (n = 5 per group). Results are the mean ± SD. * = $P < 0.05$ versus vehicle-treated controls.

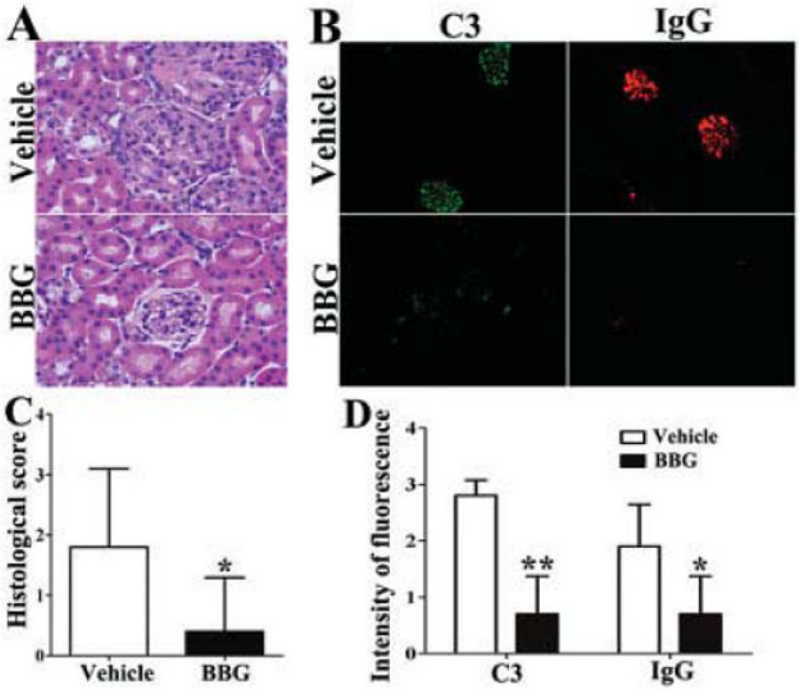

Figure 6.

Treatment of NZM2328 mice with brilliant blue G (BBG) prevents renal damage and immune complex deposition in a model of adenovirus-expressing interferon-*α*–accelerated glomerulonephritis. **A** and **C**, Formalin-fixed sections of renal tissue from vehicle-treated and BBG-treated mice were stained with hematoxylin and eosin for histopathologic assessment of the glomeruli **(A)**, and the severity of renal damage was graded by semiquantitative histologic scoring **(C)**. Original magnification × 400. **B** and **D**, Snap-frozen renal sections were stained for deposition of C3 (fluorescein isothiocyanate-conjugated) or IgG (Alexa Fluor 555–conjugated) **(B)**, and immunofluorescence microscopy was used to assess the intensity of fluorescence **(D)** after 5 weeks of BBG treatment compared with vehicle treatment. Results are the mean ± SD. * = $P < 0.05$; ** = $P < 0.01$ versus vehicle-treated controls.